Technical University of Varna Annual Journal
https://doi.org/10.29114/ajtuv.vol9.iss1.330
Vol. 9 Issue 1 (2025)
Published: 2025-06-30
ISSN 2603-316X (Online)

Methodology of accelerated testing of electrode materials based on Zn-Ni-Cu alloys for alkaline water electrolysis with the possibility of their regeneration

Danylo Savitskyi[1] and *Antonina* Maizelis[2]

1 – Municipal institution of the Kharkiv City Council "Kharkiv Lyceum No. 161 "Impulse", 61176, 35 Velozavoska Street, Kharkiv, Ukraine
2 – National Technical University "Kharkiv Polytecnic Institute", Department of Technical Electrochemistry, 61002, 2 Kyrpychova Street, Kharkiv, Ukraine
Corresponding author contact: a.maizelis@gmail.com

Abstract. *The method of accelerated tests of degradation resistance of electrodes based on Zn-Ni-Cu alloys, which simulates the operation of electrodes under the conditions of periodic changes in the load on the electrolyzer of alkaline water electrolysis is provided. It was found that during multicycling of electrodes using quasi-stationary cyclic polarization curves in the range of hydrogen evolution potentials on a multilayer electrode with alternating layers of alloys and a mixture of metals with hydroxides, the overvoltage of hydrogen evolution decreases, in contrast to a single-layer electrode, the surface of which is modified under such conditions with increasing overvoltage of hydrogen evolution. This is due to both the different degree of surface development due to the leaching of zinc from the phases of the alloy enriched with it, and to another change in the phase composition of the surface layer of the coating. In the process of long-term cycling, the corrosion potential of coatings becomes more negative, and the rate of corrosion increases. After the regeneration of the surface and repeated cycling, the activity of the electrodes is still preserved: in comparison with the initial state, there remains a decrease in the overvoltage of hydrogen evolution reaction both on a single-layer electrode (by 0.3-4.3%), and on a multilayer one (by 13.6-23.9 %). Moreover, the exchange current density of hydrogen evolution reaction increases by 2.4 times in the case of a single-layer electrode and by 1.7 times in the case of a multilayer electrode.*

Keywords: Zn-Ni-Cu alloy, multilayer coatings, catalytic activity, hydrogen evolution, resistance to degradation

1 Introduction

The alkaline version of water electrolysis allows the use of a wide range of electrode materials that are corrosion-resistant in this environment. Nickel-based materials are the most promising relatively cheap. To increase the efficiency of electrolysis, it is necessary to reduce the overvoltage of the hydrogen evolution reaction (HER), and to improve the operational properties of the electrodes [Qianfeng, 2014]. To increase the surface area of the electrode, various versions of Raney-nickel are used [Solmaz, 2024]. One of the most important parameters of an electrode with a catalytically active coating is its long-term stability [Tao, 2018]. The usual causes of electrode degradation are the reduction of the active surface, which is caused by the instability of the developed structure of the catalyst and the coating of the surface with poisons and bubbles [Malik, 2017].

Alloys of the Ni-Zn-Cu system (Cu-Ni, Cu-Zn, Ni-Zn, Zn-Ni-Cu) are also considered as electrode material. The Zn-Ni-Cu ternary alloy will be used as a material for further selective leaching of the less stable component, zinc, to obtain a porous material [Lo, 2021]. The formed porous matrix has a more positive potential. Nickel-enriched Zn-Ni-Cu electrode coatings are obtained by chemical and electrochemical deposition for further formation of electrode materials [Liu, 2019]. Also, porous coatings are obtained by galvanic replacement, when the more active component of the coating is dissolved, and ions of a more electropositive metal, which are present in the solution, are deposited on the surface of the electrode [Lo, 2023]. The developed surface of alloys of the Zn-Ni-Cu system is promising for use as cathodes in the hydrogen evolution reaction during the electrolysis of water in an alkaline environment [Maizelis, 2019].

All developed surfaces are highly sensitive to degradation of the active surface. Resistance to degradation is determined by analyzing the effects of long-term potentiostatic electrolysis [Zhao, 2022],

Technical University of Varna Annual Journal
https://doi.org/10.29114/ajtuv.vol9.iss1.330
Vol. 9 Issue 1 (2025)
Published: 2025-06-30
ISSN 2603-316X (Online)

galvanostatic load changes [Mojabi, 2022; Solmaz, 2010], step [Mojabi, 2022] and multi-cyclic [Zhao, 2022; Mojabi, 2022; Solmaz, 2010; Döşlü, 2021; Elsharkawy, 2024; Liu, 2022]. Therefore, research aimed at obtaining new cheap materials with increased catalytic activity and a developed surface, which are also stable during long-term operation, is urgent. The purpose of the work is to evaluate the advantages of a multilayer coating compared to a single-layer coating as a catalytically active coating in the hydrogen evolution reaction in an alkaline medium by means of accelerated tests under conditions simulating electrolysis with variable load.

2 Materials and methods

2.1 Electrolytes and electrodes

The electrocatalytic coating was deposited from an electrolyte containing 0.210 mol L^{-1} Ni^{2+}, 0.042 mol L^{-1} Cu^{2+}, 0.005 mol L^{-1} Zn^{2+}, 0.455 mol L^{-1} glycinate, 1.700 mol L^{-1} NH_4^+ and 5 g L^{-1} of KCl; pH 8.5. Electrode testing and determination of the corrosion rate were carried out in a 1 mol L^{-1} NaOH solution.

The coatings were deposited on "Steel 3" grade carbon steel samples with a working area of 2.25 cm^2 . Before deposition, it was cleaned of carbide with silicon paper successively with abrasiveness of 1000, 2000 and 3000 grit. A mesh electrode made of platinum was used as counter electrode. The reference electrode was Ag/AgCl electrode with saturated KCl solution, which was placed in a separate glass (the contact between the working electrode and the reference electrode was provided with a salt bridge). When testing coatings in an alkali solution, a mercuric oxide electrode was used as a reference electrode.

2.2 Electrolytes and electrodes

MTech SPG-500fast potentiostat was used for coating deposition and testing. Deposition of coatings was carried out in potentiostatic mode. The multilayer coating was deposited in the programmed potentiostatic mode: two potential values and the duration of each of them were set, as well as the number of repetitions of such a program was specified.

Testing of electrodes for resistance to degradation was carried out by multicycling in the region of hydrogen evolution potentials with a potential scan rate of 1 mV s^{-1}. Regeneration of the surface was carried out by cycling in the region of potentials of the reversible surface oxidation-reduction reaction hydroxide-oxohydroxide of nickel and copper with a potential scan rate of 50 mV s^{-1}.

Corrosion research was carried out by the polarization method. Quasi-stationary polarization curves were obtained after holding the electrode for 30 minutes in a solution without current, with a potential scan rate of 1 mV s^{-1}, from a potential that is 50 mV more positive than the open circuit potential, to the cathode side by 200-300 mV.

The corrosion current was determined by the polarization method according to the equation:

$$i_{cor} = \frac{b_k \cdot b_a}{2{,}303(b_k + b_a)R_p} \quad (1)$$

where b_a and b_k are the Tafel coefficients of the anodic and cathodic branches of the polarization curve, respectively, mV; R_p is the polarization resistance, Ω cm^2.

The activity of coated electrodes was evaluated by polarization curves, which were obtained at a potential scan rate of 1 mV s^{-1} without *iR* correction for comparison of overvoltage Δ*E* of HER at test current densities. The parameters of the kinetics of HER were determined from the polarization curves obtained at a scan rate of 1 mV s^{-1} with the *iR* correction. Tafel coefficients were calculated according to Eq. 2.

Exchange current density j_o was determined based on the Tafel equation

$$E = a + b \cdot \lg j \quad (2)$$

where *a* is the Tafel coefficient *a*, mV; *b* is Tafel coefficient *b*, mV; *j* is current density, A cm^{-2}, as

Technical University of Varna
Annual Journal
https://doi.org/10.29114/ajtuv.vol9.iss1.330
Vol. 9 Issue 1 (2025)
Published: 2025-06-30
ISSN 2603-316X (Online)

$$j_0 = 10^{-a/b} \quad (3)$$

The real surface area C_{real} of electrocatalytic electrodes was determined by the capacitive method. For this, a series of cyclic volt-ampere curves (CVAs) in 1 mol L^{-1} KOH solution was obtained at scan rate from 25 to 400 mV s^{-1} and the double layer capacity C_{dl} was determined as the slope of the curve of the capacitive current I_{dl} on the scan rate. The surface area was determined, taking into account that the capacity of the double layer for the oxidized surface of the metal is 60 μF cm^{-2}.

The elemental composition of the coatings was determined using an X-ray fluorescence spectrometer SPRUT (XRF). To display the morphology of the surface, a BIOLAM M optical microscope was used under oblique illumination with an LED flashlight.

3 Results of experiments and their discussion

3.1 Electrodeposition of coatings

Zn-Ni-Cu alloys is deposited by the potentiostatic method from an ammonia-glycinate electrolyte, which has potential regions for the deposition of alloys of different phase composition. Multilayer coating "ML" is deposited by the two-pulse potentiostatic method, by alternating layers enriched with copper and nickel, which are deposited at a potential of -1.1 V, and layers enriched with zinc and with inclusions of all metal's hydroxides, which are deposited at a potential of -1.3 V. The deposition time of each layer is until the charge reaches 0.6 C cm^{-2}. The single-layer coating "SL" is deposited at an intermediate potential between the potentials of the layers of the multilayer coating, -1.2V.

The chronoamperograms of coating deposition are shown in Fig. 1. The deposition of each layer of the multilayer coating (curve 1, Fig. 1) at a potential of -1.1 V is accompanied by an increase in the value of the current due to an increase in the surface area of the crystals. In the process of deposition of each layer of the alloy at -1.3 V, the current decreases, which may be due to difficulties in the diffusion of ions to the surface of the electrode at a significantly higher current density. At the same time, in general, during the deposition of a thick coating, the deposition current increases, which is associated with an increase in the surface area of the electrode surface.

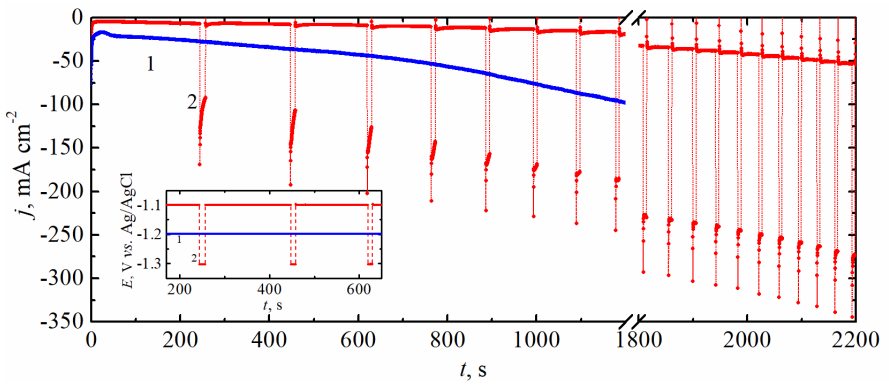

Fig. 1. Chronoamperograms of deposition of single-layer "SL" (1) and multilayer "ML" (2) coatings.

Table 1. Coating characteristics

Parameter		Coating	
		"SL"	"ML"
Mode of deposition of coatings		-1.2 V	[(-1.1 V; 0.6 C cm^{-2}) / (-1.3 V; 0.6 C cm^{-2})]$_n$
The content of metals in the original coating, wt. %	Zn	64.5	54.3
	Ni	19.6	25.6
	Cu	15.9	20.1
The content of metals in the coating after 1st cycling, wt. %	Zn	33.0	27.4
	Ni	40.0	41.6
	Cu	27.0	31.0

Technical University of Varna
Annual Journal
ISSN 2603-316X (Online)
https://doi.org/10.29114/ajtuv.vol9.iss1.330
Vol. 9 Issue 1 (2025)
Published: 2025-06-30

The composition of the obtained coatings, determined by the X-ray fluorescence method, is given in Table 1: the deposited single-layer coating has a nickel content of 19.6%, which corresponds to γ -phase of the zinc-nickel alloy. The multilayer coating turned out to be more enriched in nickel and copper.

3.2 Testing of electrodes for resistance to degradation with intermediate regeneration

To determine the stability of electrodes under conditions of electrolysis with variable load, they were multi-cycled in the potential range corresponding to a wide range of current densities, i.e., from 0 mA cm^{-2} to 150 mA cm^{-2}. Unlike known multi-cycling variants [Liu, 2022], CVAs were obtained with a much lower potential scan rate with a corresponding decrease in the number of cycles, which is close to real conditions. Cycling was performed only in the cathodic potential region, without entering the anodic region, in which hydrogen is oxidized. Therefore the test conditions are mitigated by reducing the blocking of surfaces by hydrogen bubbles. In addition, cycling was limited not to the potential value, which, during degradation accompanied by a decrease in current values, reduces the load on the electrode, but was performed to the same current values. Such quasi-stationary CVAs in 1 mol L^{-1} NaOH are shown in Fig. 2. It should be noted that with an increase in the number of cycles during the first cycling (the first 22 cycles), the CVAs on the single-layer electrode shift towards more negative values (Fig. 2a, the CVAs series is marked in blue), as on all nickel-containing electrodes [Zhao, 2022], and on the multilayer electrode CVAs shift towards more positive values (Fig. 2b), as on the Cu-Ni-Zn alloy [Solmaz, 2010]. This reduction in the overvoltage of HER on a multilayer electrode is probably due to both a more significant increase in surface area due to zinc dissolution and a greater enhancement of catalytic activity due to a different change in the elemental and phase composition of the surface coating layer.

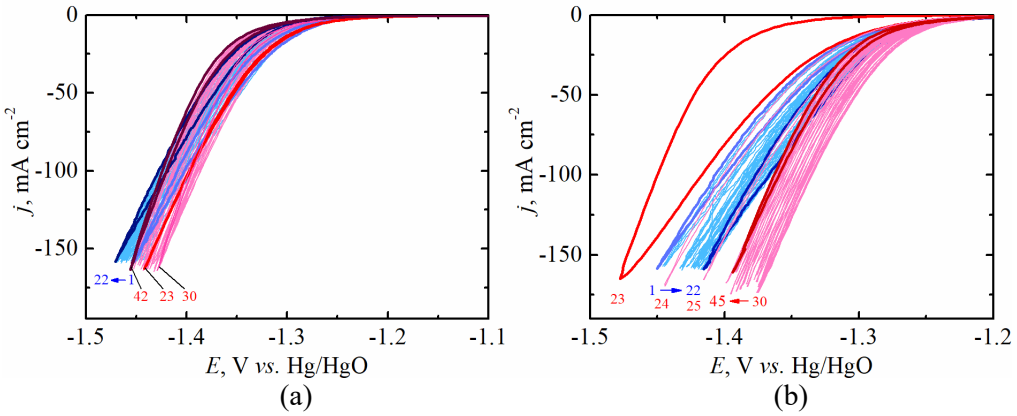

Fig. 2. 1st (cycles 1-22, blue color) and 2nd (cycles 23-45, red color) CVA series in 1 mol L^{-1} KOH on steel electrodes with single-layer (a) and multilayer (b) coatings. The potential scan rate is 1 mV s^{-1}.

Figure 3 shows the dependences of the potentials of hydrogen evolution at current density of 100 mA cm^{-2} on the cycle number, which are obtained from the data of the direct run of the CVAs in Fig. 2, which describe in more detail the change in HER overvoltage. In particular, periodic changes are observed (curve 1), which may be associated with the periodic detachment of hydrogen bubbles.

The morphology of the electrode surface after cycling reveals a more uniform distribution of dendrites in the case of the multilayer coating (Fig. 4b). The zinc content in the coatings decreased by approximately half and the nickel and copper content increased by one and a half times (Table 1).

3.3 Regeneration of catalytic activity of coatings

Since the catalytic activity of the surface, which allows the inclusion of metal hydroxides, depends on their surface concentration, an attempt was made to increase it by cycling the electrodes in the potential region of the oxohydroxide-hydroxide transition (Fig. 5). The number of seats of both electrodes increases with increasing cycles. The height of the peaks on the surface of the multilayer electrode is greater (Fig. 5 b), which indicates a greater specific number of active centers on its surface in terms of the geometric surface area.

Technical University of Varna
Annual Journal
ISSN 2603-316X (Online)
https://doi.org/10.29114/ajtuv.vol9.iss1.330
Vol. 9 Issue 1 (2025)
Published: 2025-06-30

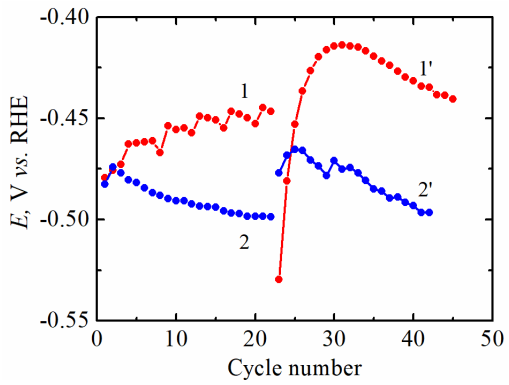

Fig. 3. Change in hydrogen evolution potentials with a current density of 100 mA cm^{-2} during cycling on multilayer (1) and single-layer (2) electrodes in 1st (1, 2) and in the 2nd (1', 2') series of CVAs.

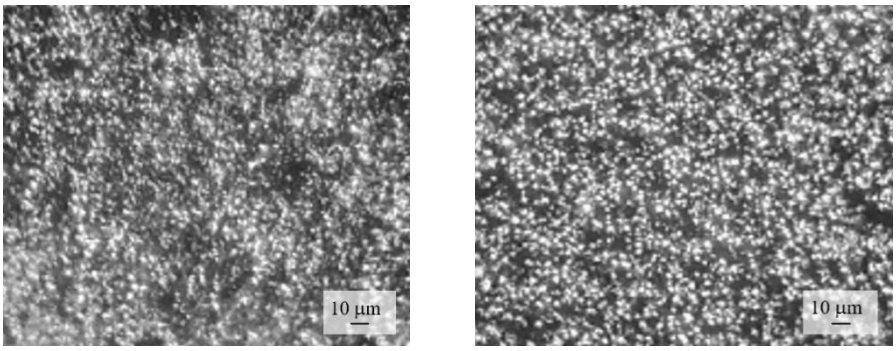

Fig. 4. Surface morphology of single-layer (a) and multilayer (b) electrodes after cycling.

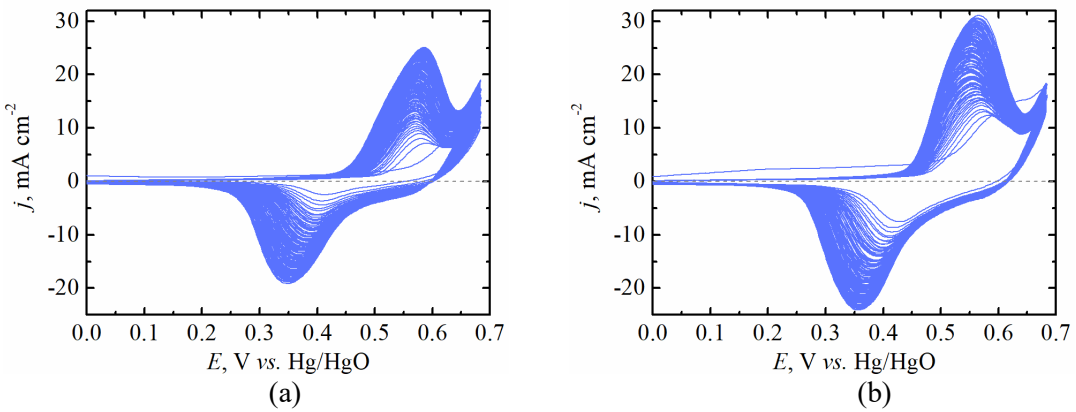

Fig. 5. CVAs on single-layer (a) and multilayer (b) electrodes in 1M NaOH.

Determination of the real surface area of the electrodes by the capacitive method by cycling in the non-Faraday region of potentials (Fig. 6) revealed a significantly more developed surface of the multilayer electrode (53 cm^2 and 81 cm^2 for single-layer and multilayer electrodes).

After regeneration in the region of the potentials of the hydroxide-oxohydroxide transition, the corrosion potential in the alkaline solution is -378 mV according to the Hg/HgO reference electrode (Fig. 4, Fig. 7a), the corrosion rate is minimal. In the process of the subsequent, 2nd cycle, oxo-compounds on the surface of the electrode are restored in the region of hydrogen evolution potentials, and the corrosion potential shifts toward negative values (curves 1-3). At the same time, the increase in the

Technical University of Varna
Annual Journal
https://doi.org/10.29114/ajtuv.vol9.iss1.330
Vol. 9 Issue 1 (2025)
Published: 2025-06-30
ISSN 2603-316X (Online)

corrosion current indicates a significant increase in the degree of degradation of the electrode by the end of the 2nd cycle (curve 1).

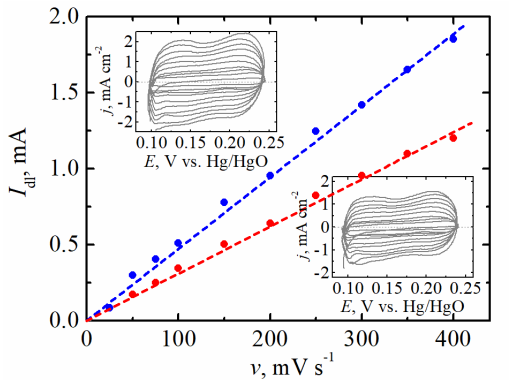

Fig. 6. C_{dl} profiles of multilayer (1) and single-layer (2) electrodes.

At the same time, the CVAs of the 2nd series (Fig. 2a, cycles 23-42, red color) continue to shift to the region of negative potential values. With a more accurate examination of the overvoltage change, for example, at 100 mA cm^{-2} (curve 2' of Fig. 3), it can be concluded that after the regeneration of the electrode, the overvoltage practically returned to the initial level before the first cycling, but during the 2nd cycling again increased. In the case of a multilayer electrode, after regeneration in the first cycle of the 2nd series of CVAs (Fig. 2, red color), the surface was activated with difficulty, but then, by the 30th cycle, the CVA shifted towards the maximum reduction of the overvoltage of HER, and only after this did the multilayer electrode degradation process begin. The overvoltage begins to grow (curve 1', Fig. 3), but does not exceed the values of the 1st series of CVAs (curve 1).

With each series of cycling, the corrosion potential (Fig. 7b) in comparison with the initial value (Fig. 1) shifts, due to the dissolution of the most active component Zn, towards positive values with a decrease in the corrosion current. This means that the corrosion potential of the original coating (-1.12 V) is significantly more positive compared to the potential of zinc in this environment (-1.5 V), what indicates the absence of free zinc in the coating composition.

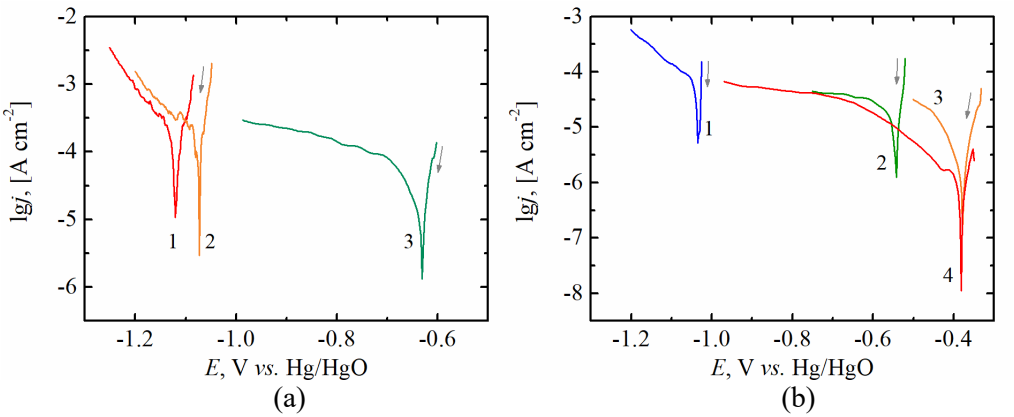

Fig. 7. Corrosion diagrams (a) of a single-layer coating after regeneration (4) and during the 2nd cycle: after the 29th cycle (3), after the 37th cycle (2) and after the 42nd cycle (1) and (b) multilayer coating before cycling (1), after the 1st cycling (2) and after the 2nd (3)

3.4 Change in the kinetic parameters of the HER in the process of tests on the stability of electrodes with intermediate regeneration

Figure 8 shows the cathodic polarization curves of hydrogen evolution on single-layer (Fig. 8a) and multilayer (Fig. 8b) electrodes before cycling in an alkali solution (curve 1), after the 1st cycling (curve

Technical University of Varna
Annual Journal
ISSN 2603-316X (Online)
https://doi.org/10.29114/ajtuv.vol9.iss1.330
Vol. 9 Issue 1 (2025)
Published: 2025-06-30

2) and after regeneration and the 2nd cycling (curve 3). Unlike multicycling under conditions of surface saturation with hydrogen (Fig. 2), the cathodic polarization curves on both electrodes shift towards positive potential values. A more significant shift of the curves on the multilayer electrode (Fig. 8b) indicates its greater resistance to degradation. The values of the hydrogen evolution overvoltage at some current densities are given in Table 2. The results of the analysis of these curves in semi-logarithmic Tafel coordinates with *iR* correction (Fig. 8c and Fig. 8d) are given in Table 2.

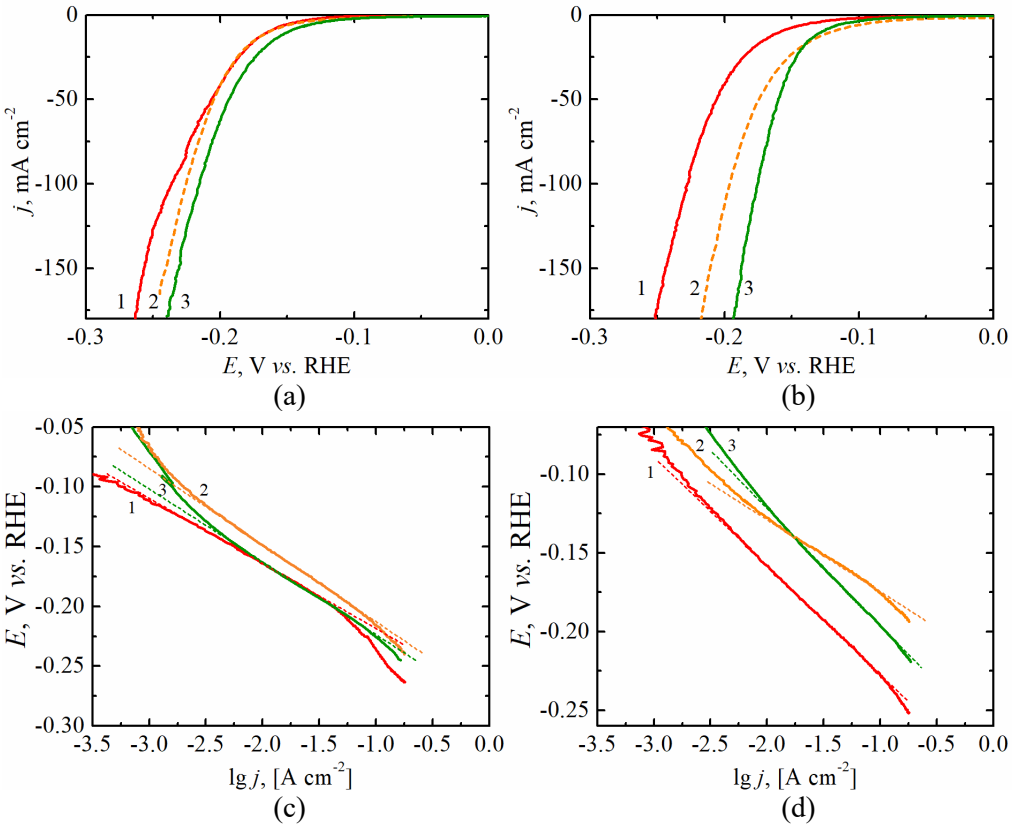

Fig. 8. Cathodic polarization curves of hydrogen evolution (a, b) and corresponding Tafel plots with *iR* correction (c, d) on single-layer (a, c) and multilayer (b, d) electrodes before cycling (1), after the 1st cycling (2) and after the second cycling (3)

Table 2. Kinetic parameters of the hydrogen evolution reaction

Kinetic parameter	Coating	Before cycling	After the 1st cycle	After regeneration and the 2nd cycle
a, mV	"SL"	-273	-282	-287
	"ML"	-297	-224	-245
b, mV	"SL"	55	66	62
	"ML"	69	48	61
$i_{o(geom)}$, μA cm^{-2}	"SL"	9.9	56.2	23.3
	"ML"	52.5	22.5	89.7
$i_{o(real)}$, μA cm^{-2}	"SL"	0.19	1.06	0.44
	"ML"	0.65	0.28	1.11
ΔE (10 mA cm^{-2}), mV	"SL"	-164.2	-149.7	-163.7
	"ML"	-158.4	-128.2	-120.5
ΔE (50 mA cm^{-2}), mV	"SL"	-206.5	-193.5	-204.7
	"ML"	-206.1	-160.4	-174.2
ΔE (100 mA cm^{-2}), mV	"SL"	-236.8	-215.2	-226.7
	"ML"	-228.1	-176	-197

After the first cycle (Fig. 9a), depending on the current density, there is a decrease in HER overvoltage on a single-layer electrode by 6.3-9.1% (left columns), and on a multilayer one by 19.1-22.8% (right

Technical University of Varna
Annual Journal
ISSN 2603-316X (Online)
https://doi.org/10.29114/ajtuv.vol9.iss1.330
Vol. 9 Issue 1 (2025)
Published: 2025-06-30

columns). After doubling the cycling time (Fig. 9b), through to the regeneration of the electrodes, this indicator of activity is still better, compared to the initial state. The decrease in overvoltage on the single-layer electrode (increase by 0.3-4.3%, left columns), and on the multilayer electrode (increase by 13.6-23.9%, right columns).

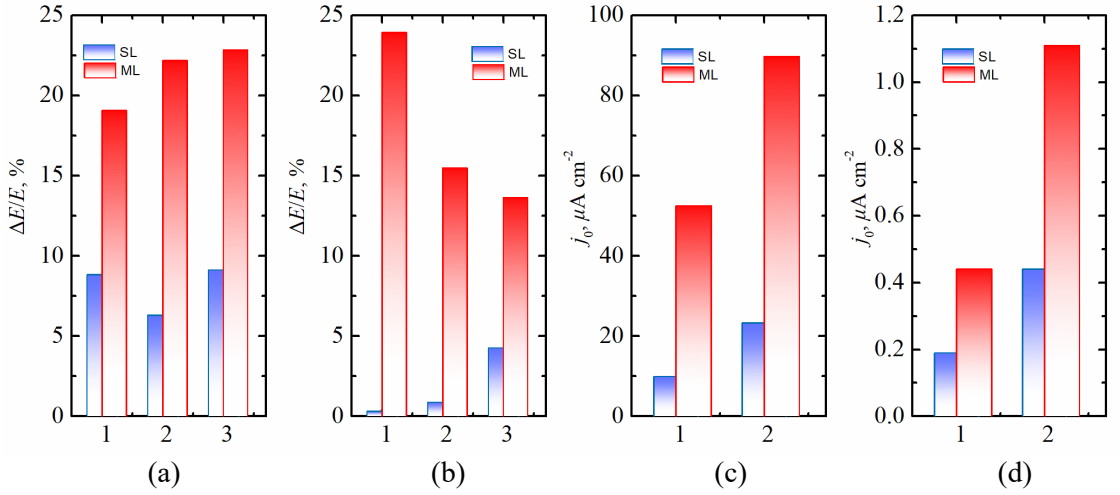

Fig. 9. (a, b) Relative reduction of HER overvoltage at a current density of 10 mA cm^{-2} (1), 50 mA cm^{-2} (2) and 100 mA cm^{-2} (3) after the 1st (a) and 2nd (b) cycling of a single-layer (left columns) and multilayer (right columns) electrodes. (c, d) exchange current before (1) and after (2) cycling, taking into account the geometric (a) and real (b) surface area

The exchange current density of the HER (Fig. 9c) after cycling increases on a single-layer electrode from 9.2 μA cm^{-2} to 23.3 μA cm^{-2} (left columns), on a multilayer one it is from 52.5 μA cm^{-2} to 89.7 μA cm^{-2} (right columns). Since the advantage of the multilayer electrode is preserved when converted to the real surface area (Fig. 9d), it is caused not only by the development of the surface, but also by its greater catalytic activity due to another change in composition compared to a single-layer electrode.

4 Conclusions

The method of accelerated tests of resistance to degradation of electrodes based on Zn-Ni-Cu alloys, which in a complex with the control of the surface morphology, its corrosion resistance and parameters of the HER, includes multicycling using quasi-stationary cyclic voltage-current curves in the area of hydrogen evolution, is closer to real operating conditions of electrodes in conditions of periodic load changes in comparison with fast multicycling.

A multilayer coating deposited by a two-pulse potentiostatic method from an ammonia-glycinate electrolyte on carbon steel electrodes, compared to a single-layer coating deposited at a potential intermediate between the potentials of the deposition of the layers of the multilayer coating, is more enriched in nickel and copper and has a 1.5 times larger real area surface, the exchange current density of the HER on its surface is greater by 5.3 times, and hydrogen is produced on it with a lower overvoltage of 9 mV at a test current density of 100 mA cm^{-2} .

In the process of long-term cycling the corrosion potential of the electrode surface becomes more negative, and the corrosion rate increases, which accelerates its degradation. It was found that when the electrode is cycled in the range of hydrogen evolution potentials, the HER overvoltage on the multilayer electrode decreases, in contrast to the single-layer electrode, the surface of which is modified under such conditions with increasing HER overvoltage.

Regeneration of electrodes by cycling in the region of the hydroxide-oxohydroxide transition increases the number of hydroxo-groups on the surface, their degradation slows down.

After repeated cycling, the activity of the electrodes is still preserved: in comparison with the initial state, there is a decrease in overvoltage both on the single-layer electrode (by 0.3-4.3%), and on the

https://doi.org/10.29114/ajtuv.vol9.iss1.330
Vol. 9 Issue 1 (2025)
Published: 2025-06-30
ISSN 2603-316X (Online)

multilayer one (by 13.6-23.9%). In addition, the exchange current density of the HER also increases, by 2.4 times in the case of the single-layer electrode and by 1.7 times in the case of the multi-layer electrode.

The advantage of a multi-layer coating is associated with both a more significant increase in surface area due to the leaching of zinc from alloy phases enriched with it in the process of long-term electrolysis in an alkaline environment, and with an increase in its catalytic activity due to another change in the phase composition of the surface layer of the coating.

References

Döşlü S.T., Döner A., Yıldız R. (2021) Electrocatalysis properties of CuZn electrode with Pt and Ru decoration. *International Journal of Hydrogen Energy*, 46(43), 22409-22421. https://doi.org/10.1016/j.ijhydene.2021.04.064

Elsharkawy S., Kutyła D., Marzec M.M., Zabinski P. (2024) Electrodeposition of hydrophobic Ni thin films from different baths under the influence of the magnetic region as electrocatalysts for hydrogen production. *International Journal of Hydrogen Energy*, 61, 873-882. https://doi.org/10.1016/j.ijhydene.2024.03.045

Liu B., Li Z. (2019) Electrochemical treatment of a smooth Cu-Ni-Zn surface into layered micro-chips of rice grain-like Cu/Ni$(OH)_2$ nanocomposites as a highly sensitive enzyme-free glucose sensor. *Journal of Electroanalytical Chemistry*, 855, 113493. https://doi.org/10.1016/j.jelechem.2019.113493

Liu W., Tan W., Yang Y., He H. (2022) One-step galvanostatic electrodeposition of Ni-Se-Dy film on Ni foam for hydrogen evolution reaction in alkaline solution. *Journal of Alloys and Compounds*. 925, 166706. https://doi.org/10.1016/j.jallcom.2022.166706

Lo N.C., Sun I.W., Chen P.Y. (2021) Electrochemical preparation of porous ZnCuNi by electrodeposition in ethanolic deep eutectic solvent followed by anodic or cathodic dealloying in alkaline aqueous solutions for higher nitrate reduction activity. *Journal of Electroanalytical Chemistry*, 2021, 890, 115256. https://doi.org/10.1016/j.jelechem.2021.115256

Lo N.C., Yu C.L., Chen P.Y. (2023) Characterization of Nanowire-Constructed Porous CuZn and Cu-NiZn Nitrate-Active Electrodes Prepared via Galvanic Displacement on Electrodeposited Zn Templates in Ionic Liquids. *Journal of Electronic Materials*, 52(5), 2995-3007. https://doi.org/10.1007/s11664-023-10279-z

Maizelis A., Bairachniy B. (2019) Formation of multilayer metal-hydroxide electrode with developed surface for alkaline water electrolysis. Materials Today: Proceedings, 6, 227-231. https://doi.org/10.1016/j.matpr.2018.10.098

Malik B., Anantharaj S., Karthick K., Pattanayak DK, Kundu S. (2017) Magnetic CoPt nanoparticle-decorated ultrathin Co(OH) 2 nanSLeets: an efficient bi-functional water splitting catalyst. *Catalysis Science & Technology*, 7(12), 2486-2497. https://doi.org/10.1039/C7CY00309A

Mojabi S., Sanjabi S. (2022) Decorated fractal Ni-Cu foam with Pd nanoparticles as a high-performance electrocatalyst toward hydrogen evolution reaction. *Thin Solid Films*, 758, 139415. https://doi.org/10.1016/j.tsf.2022.139415

Qianfeng L., Wang E. & Sun G. (2014) Layered transition-metal hydroxides for alkaline hydrogen evolution reaction. *Chinese Journal of Catalysis*, 41(4), 574-591. https://doi.org/10.1016/S1872-2067(19)63458-3

Solmaz R. (2024) Electrochemical preparation, characterization, and application of a novel cathode material, mild Steel/Ni/NiZn-Pt, for alkaline water electrolysis. *Energy Sources, Part A: Recovery,*

https://doi.org/10.29114/ajtuv.vol9.iss1.330
Vol. 9 Issue 1 (2025)
Published: 2025-06-30
ISSN 2603-316X (Online)

Utilization, and Environmental Effects, 36(11), 1212-1218. https://doi.org/10.1080/15567036.2010.545804

Solmaz R., Döner A., Kardaş G. (2010) Preparation, characterization and application of alkaline leached CuNiZn ternary coatings for long-term electrolysis in alkaline solution. *International journal of hydrogen energy*, 35(19), 10045-10049. https://doi.org/10.1016/j.ijhydene.2010.07.145

Tao S., Yang F., Schuch J., Jaegermann W., Kaiser B. (2018) Electrodeposition of nickel nanoparticles for the alkaline hydrogen evolution reaction: correlating electrocatalytic behavior and chemical composition. *ChemSusChem*, 11 (5), 948-958. https://doi.org/10.1002/cssc.201702138

Zhao, Y., Wei, S., Xia, L., Pan, K., Zhang, B., Huang, Dong Z., Wu HH, Lin J., Pang H. (2022) Sintered Ni metal as a matrix of robust self-supporting electrode for ultra-stable hydrogen evolution. *Chemical Engineering Journal*, 430, 133040. https://doi.org/10.1016/j.cej.2021.133040